Analyzing Type IIn Supernovae spectra to determine if some arise from runaway stars

A THESIS
SUBMITTED TO THE FACULTY OF THE GRADUATE SCHOOL
OF THE UNIVERSITY OF MINNESOTA
BY

Michael Makmur

IN PARTIAL FULFILLMENT OF THE REQUIREMENTS
FOR THE DEGREE OF
MASTER OF SCIENCE

Patrick L. Kelly

May, 2020

Acknowledgements

tbd

The data presented herein were obtained at the W. M. Keck Observatory, which is operated as a scientific partnership among the California Institute of Technology, the University of California and the National Aeronautics and Space Administration. The Observatory was made possible by the generous financial support of the W. M. Keck Foundation.

The author wishes to recognize and acknowledge the very significant cultural role and reverence that the summit of Maunakea has always had within the indigenous Hawaiian community. We are most fortunate to have the opportunity to use observations from this mountain.

This research has made use of the Keck Observatory Archive (KOA), which is operated by the W. M. Keck Observatory and the NASA Exoplanet Science Institute (NExScI), under contract with the National Aeronautics and Space Administration.

Dedication

tbd

Abstract

We have analyzed observations of Type IIn supernovae taken by the DEIMOS spectrograph on Keck II in order to determine if there is a significant offset in the peak of the SN Hα emission with respect to the predicted Hα peak wavelength of the host galaxy at the SN position along the slit. An offset of 30 km s^{-1} or greater may imply a runaway progenitor star, ejected via dynamical interaction or as the mass-gaining companion of a binary star system where the primary explodes first. Significant fractions of runaway progenitors would have an impact on our understanding of the progenitors of SNe IIn, and seeing as luminous blue variable (LBV) stars are commonly considered as a progenitor star it could also have impacts on the evolutionary path for LBV stars. LBVs are not seen in evolution models as an end-of-life stage but rather a transition stage, and they are also not expected to be the result of a binary supernova kick.

Spectra and resulting offset velocities were analyzed and computed for six SNe IIn, of which two returned as possible runaway candidates. Of these two, the site of SN 2010jl had direct observations by the Hubble Space Telescope approximately 10 years prior to explosion. These observations show a luminous blue source in pre-explosion imaging, which was theorized to either be an extremely bright and young star cluster or a massive luminous blue variable star. The other runaway candidate, SN 2013dz, does not appear in the literature but shows signatures of an asymmetrical circumstellar medium. The remaining four SNe IIn show no significant evidence of runaway behavior along the line of sight. This lack of sufficient offset velocity could imply that the progenitors did not undergo a BSS ejection, or it could alternatively imply that the progenitor gained so much mass that the resulting ejection velocity was small.

With a sample size of six observations, it is difficult to make any statistically significant conclusions. More observations of progenitors, SNe, and post-SNe regions are needed to reach a more robust conclusion.

Contents

Acknowledgements **i**

Dedication **ii**

Abstract **iii**

List of Tables **vi**

List of Figures **vii**

1 Introduction **1**

1.1 Supernovae 1

1.1.1 Type IIn Supernovae 2

1.2 Luminous Blue Variables 6

1.3 Runaway Stars 7

1.3.1 LBV Runaways as Possible SNe IIn Progenitors 8

1.4 This thesis 13

2 Observations **14**

2.1 Observed SNe IIn 14

2.2 DEIMOS 14

2.3 Hα λ6563 16

3 Analysis **18**

3.1 Reducing DEIMOS Images 18

3.2 Analyzing Velocities of SNe IIn 19

3.2.1 Limitations and Uncertainties 20

4 Discussion **24**

4.1 Runaway Candidates 24

4.1.1 SN 2010jl 24

4.1.2 SN 2013dz 26

4.2 Implications on progenitors 28

5 Conclusion **30**

5.1 Future Work 31

Appendix A. Glossary and Acronyms **36**

A.1 Glossary 36

A.2 Acronyms 38

Appendix B. Images and Spectra **39**

List of Tables

2.1 Table of observations 15
3.1 List of SNe IIn, the FWHM of their Hα emission, and their offset velocities from their host galaxies. 23
A.1 Acronyms 38

List of Figures

1.1 Cartoon of the basic structure for a SN IIn 3
1.2 Plot comparing mass-loss rate and wind velocities of SN IIn to possible progenitors 5
1.3 Plot depicting how far a runaway star will travel before exploding in a SN 9
1.4 Cumulative fraction versus distance to nearest O-type star for several stellar types from Smith and Tombleson (2015) 10
1.5 Cumulative fraction versus distance to nearest O-type star for LBVs in the Magellanic clouds from Humphreys et al. (2016) 12
2.1 Image of SN 2010jl from DEIMOS 15
2.2 Spectrum of the Hα emission from SN 2008en 16
2.3 Hα emission from SN 2013dz and its host galaxy 17
3.1 Lorentzian Fits of SN 2005R, SN 2008en, and SN 2010jl 21
3.2 Lorentzian Fits of SN 2012ab, SN 2013dz, and SN 2013W 22
4.1 SN 2010jl Hα emission relative to host galaxy 25
4.2 SN 2013dz Hα emission relative to host galaxy 27
B.1 SN 2005R Hα relative to host galaxy 39
B.2 SN 2008en Hα relative to host galaxy 40
B.3 SN 2010jl Hα relative to host galaxy 40
B.4 SN 2012ab Hα relative to host galaxy 41
B.5 SN 2013dz Hα relative to host galaxy 41
B.6 SN 2013W Hα relative to host galaxy 42

Chapter 1

Introduction

1.1 Supernovae

When stars reach the end of their lives, they will either go out with a bang or a whimper, depending on their initial masses. Stars that are born with an initial mass less than 8 solar masses ($M_\odot$) tend to fall into the latter category, releasing their outer layers into a planetary nebula and leaving their core as a white dwarf star. Stars more massive than $8M_\odot$, on the other hand, fall in the former category. These stars will undergo a sudden core collapse, with the resulting explosion ejecting several solar masses of outer layers at extreme speeds while the core collapses into a neutron star or, if massive enough, a black hole. These events are called supernovae (SNe, singular: supernova/SN), and can some of the most luminous transient events in astronomy.

There are two main types of SNe, distinguished by the presence or lack of hydrogen in their spectra - Type I SNe lack hydrogen emission while Type II have it present. Each type is further divided into subtypes.

Type I SNe are divided between Type Ia which has a silicon absorption feature, while Types Ib/c lack the Si II feature.[1] Type Ia SNe are significant as they are the result of the thermonuclear explosion of white dwarf stars. If a white dwarf star accretes enough mass to approach the Chandrasekhar mass ($1.44M_\odot$), it will re-ignite nuclear fusion and explode. There may be a binary white dwarf progenitor channel for forming Type Ia SNe as well.

[1] These are further split based on the presence of a He I line at 5876 Å.

Type II SNe are divided in four main ways:

- Type IIb SNe lose their hydrogen emission over time and their spectra begin to show similarities to Type Ib SNe (with the presence of He I 5876 Å).
- Type IIn SNe show narrow lines of hydrogen emission.
- Type II-L SNe show a linear decrease in their light curve, and have no narrow lines.
- Type II-P SNe show an extended period of luminosity (a "plateau" in their light curve, hence the "P") before decreasing in brightness.

In this thesis we take a specific eye towards Type IIn SNe.

1.1.1 Type IIn Supernovae

Type IIn supernovae (SNe IIn) are a subclass of CCSNe which show strong, narrow Balmer lines of hydrogen in their spectra (Schlegel, 1990), and make up approximately 10% of all CCSNe. It is expected that these narrow lines arise from the SN shock interacting with a dense, pre-existing circumstellar medium (CSM) surrounding the progenitor star (Smith, 2017). Some sort of extreme mass-loss is required in the decades prior to the explosion in order to generate such a CSM.

Because of the dense, surrounding CSM, the basic structure of a SNe IIn differs significantly from other SNe. As seen in Fig. 1.1, Smith (2017) splits the SN IIn into four physical zones: the unshocked CSM (1), the shocked CSM (2), the shocked SN ejecta (3), and the freely expanding SN ejecta (4). At the boundaries of each zone are the forward and reverse shocks, as well as the cold dense shell (CDS) between zones 2 and 3. In a non-SNe IIn, an observer would see radiation emerging almost entirely from zone 4, but since the CSM is so dense for these explosions, each zone can provide significant contributions towards emitted radiation (Smith, 2017). In early times when the photosphere is still in zone 1, radiation from the shock is electron scattered by the photosphere and unshocked CSM, creating narrow Hα emission lines with broad Lorentzian wings (Smith, 2017). As the explosion progresses and the photosphere recedes into zones 2 and 3, the gas piled into the CDS is constantly reheated by the shock and emits strong Hα intermediate-width lines.

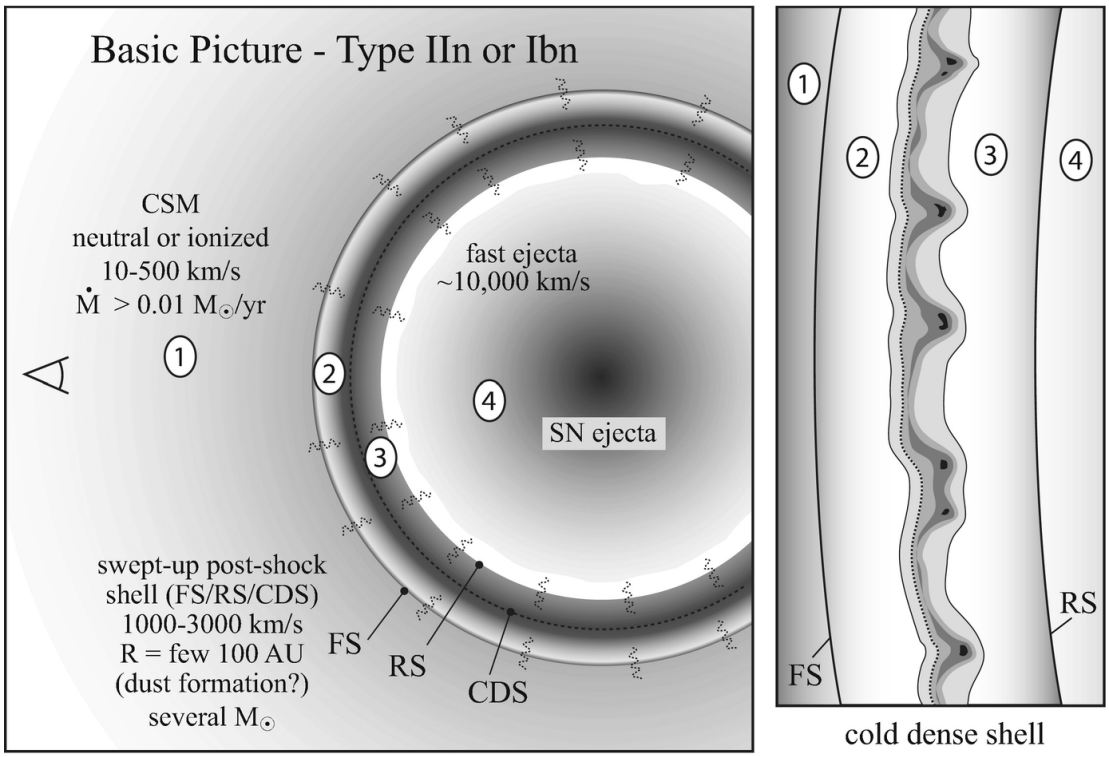

Figure 1.1: Cartoon of the basic structure of a SNe IIn. SNe IIn can be split into four separate zones: (1) the unshocked CSM, (2) the shocked CSM, (3) the shocked SN ejecta, and (4) freely expanding SN ejecta. At each boundary is a different event: between (1) and (2) exists the forward shock, between (2) and (3) is the cold dense shell (CDS), and between (3) and (4) is the reverse shock. X-rays and UV radiation can also be generated by the shock and propagate forwards into the CSM or back into the SN ejecta, and this is represented by the squiggly lines. This figure is from Smith et al. (2008).

It is important to remember that SNe IIn are an *external* phenomenon - they may actually mask other types of supernovae. Any type of core collapse supernova or even thermonuclear supernova can create the narrow Balmer lines seen in SNe IIn, so long as there is a dense enough hydrogen-rich medium surrounding the explosion (Smith, 2017). Because of this, it is impossible to trace all SNe IIn to a single type of progenitor star or explosion type. A SN IIn could be covering up a SN II-b, II-L, or II-P, and because of the dense CSM it is impossible to know what the explosion type truly is. There are also Type Ibn SNe (referenced in Fig. 1.1) which display prominent narrow helium lines, as well as Type Ia-CSM SNe which show signs of a dense CSM surrounding the thermonuclear SNe.

The luminosity of an SN IIn can be used to obtain information about the mass-loss rate of the progenitor star (Smith, 2017), allowing observers to determine other properties of the progenitor. SNe IIn can end up being much more luminous than other SNe, as the radiative shock from CSM interaction is extremely efficient at transforming the kinetic energy of the SN shockwave into visible-wavelength light (Smith, 2017). Because the luminosity is directly tied to the CSM, it can be expressed as

$$L = \frac{1}{2} w V_{\mathrm{CDS}}^3 \tag{1.1}$$

where w represents the wind density parameter, $w = \dot{M}/V_{\mathrm{CSM}}$ (where $\dot{M}$ is the mass-loss rate and V_{CSM} is the speed of the circumstellar medium), and V_{CDS} is the speed of the cold dense shell, the contact discontinuity where the SN shock and CSM meet (Smith, 2017). V_{CDS} can be estimated from the full width half maximum (FWHM) of intermediate-width lines in the optical spectrum, while V_{CSM}, the velocity of the CSM untouched by the SN shock, can be measured from narrower components. Combining this together, the mass-loss rate of the progenitor can be estimated by

$$\dot{M}_{\mathrm{CSM}} = 2L \frac{V_{\mathrm{CSM}}}{V_{\mathrm{CDS}}^3}. \tag{1.2}$$

One major caveat to this equation is that it requires a constant mass-loss rate and V_{CSM} over time in order to have the CSM density decrease as r^{-2}. If Eq. 1.2 is used when the CSM density profile is shallower, it will return a much larger mass-loss rate than is true (Dwarkadas, 2011). A review by Dwarkadas (2011) of several SNe IIn show that their mass-loss rates were overestimated, adding further confusion as to what the

progenitors to these explosions are. Additionally, many SNe IIn show signs of significant asymmetries in their CSM, which will further alter the discrepancies between the results from the equation and the actual star.

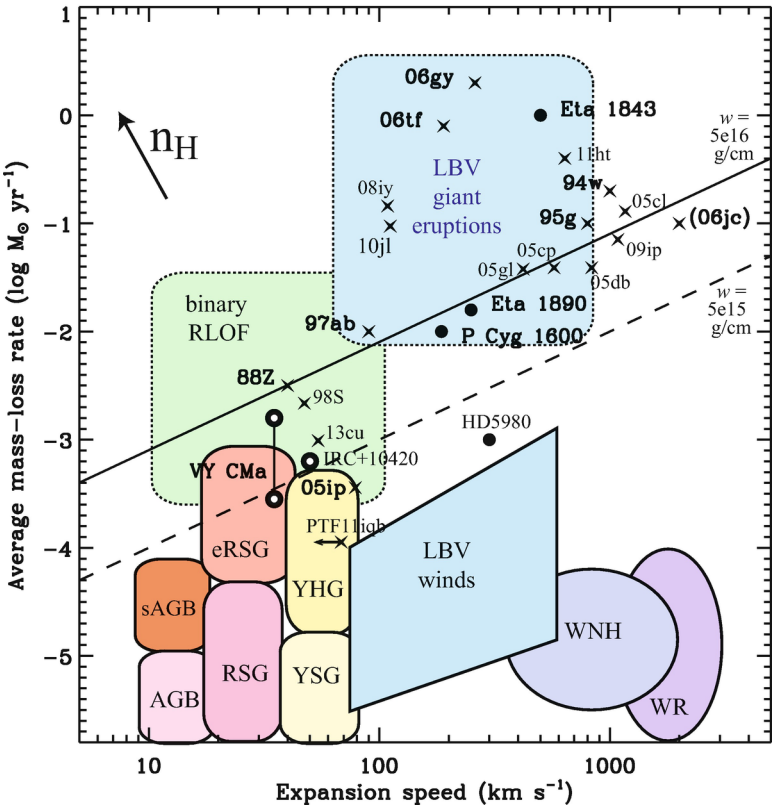

Figure 1.2: Plot of mass-loss rate as a function of wind velocity, with comparisons to known SNe IIn explosions and possible progenitor stars. Observational estimates of different SNe IIn are represented by X's, and some stars with high mass-loss (e.g. η Car) are represented by circles. The patches represent the approximate parameter spaces for different types of stars. Represented in this plot are asymptotic giant brach (AGB) and super-AGB (sAGB) stars, red supergiant (RSG) and extreme-RSGs, yellow super- and hypergiants (YSG, YHG), winds and eruptions from luminous blue variables (LBVs), Wolf Rayet stars (WR, WNH), as well as progenitors arising from basic binary Roche lobe overflow (RLOF). This figure is from Smith (2017).

Even with this setback, conclusions can be made about what kind of stars are able to produce fast enough winds and high enough mass-loss rates seen in SNe IIn. A plot from Smith (2017) comparing mass-loss rate and wind velocities of several SNe IIn and

comparing them to progenitor properties can be seen in Fig. 1.2. It is worth noting that most SNe IIn require some sort of giant luminous blue variable star (LBV) eruption in the decades preceding explosion to create enough CSM to form the narrow lines present in SNe IIn.

1.2 Luminous Blue Variables

Luminous blue variable stars (sometimes referred to as S Doradus variables) are extremely luminous, evolved, and unstable massive stars near the Eddington limit[2] which undergo irregular eruption events (Humphreys and Davidson, 1994). LBVs have a higher luminosity to mass ratio (L/M) than a typical star, as well as a larger Eddington factor ($\Gamma = L/L_{\rm Edd} > 0.5$).

When in their eruptive phase, LBVs can create a large amount of dense ($N \sim 10^{11}$ cm^{-3}), cool ($7000-9000$ K) CSM surrounding the star (Humphreys and Davidson, 1994). The most explosive of these eruptions (such as η Car and SN 2009ip[3]) can be luminous enough to be misinterpreted as SNe (known as supernova imposters). LBVs can also have a quiescent phase with decreased mass-loss and temperatures of 12,000 to 30,000 K (Humphreys and Davidson, 1994). In this visual minimum, LBVs can resemble hot supergiants or Of/WN stars.

Two main classes of LBVs may exist with completely separate evolutionary histories (Humphreys et al., 2016). "Classical" LBVs originate from stars with initial masses ($M_{\rm ZAMS}$) greater than $50 M_\odot$ and have bolometric magnitudes between -9.7 and -11.5 mag. Their high mass-loss rates means that they lose mass too quickly to cool and become a red supergiant (RSG). Making up the second class are less luminous LBVs, originating from stars in the range of 25 to 40 $M_\odot$ and have bolometric magnitudes of -8 to -9.5 mag. These stars are expected to have completed their RSG stage and moved back towards the blue end of the H-R diagram, passing through an LBV phase where they lose up to half of their initial mass (Humphreys et al., 2016). This mass-loss allows such stars to achieve an L/M similar to the more luminous LBVs.

Traditionally the more massive LBVs serve as a transition stage between an O-type

[2] The *Eddington limit* is the maximum luminosity an object can have while still maintaining hydrostatic equilibrium, the balance between gravitational pull inwards and radiation pressure outwards.

[3] SN 2009ip actually exploded as an SN IIn in 2012, though this is debated (Mauerhan et al., 2012).

star to a hydrogen-poor Wolf-Rayet (WR) star (Smith and Owocki, 2006). For massive, classical LBVs, the evolutionary path is

$$\text{O} \rightarrow \text{WNL (H-rich)} \rightarrow \text{LBV} \rightarrow \text{WN (H-poor)} \rightarrow \text{WC}$$

where the LBV plays the role of ejecting the WNL star's H-rich envelope (Langer et al., 1994; Gräfener and Hamann, 2008). In order to reconcile that the direct progenitor of a SNe IIn is not an LBV, Dwarkadas (2011) suggest a very short WR phase or a clumpy CSM to create the necessary CSM properties, but the general consensus in the literature is that LBVs mysteriously serve as the main progenitor.

Referring back to Fig. 1.2, we see that while some SNe IIn could arise from binary Roche lobe overflow (RLOF) or extreme red supergiants (eRSGs), it is clear that mass-loss estimates and wind speeds favor an LBV progenitor for most SNe IIn. Indeed, direct observations of progenitors for SNe IIn explosions such as SN 2009ip (Mauerhan et al., 2012, still debated) and SN 2010jl (Smith et al., 2011) appear to show a progenitor LBV in the location of the future explosion, though follow up observations to see if they are just SN imposters are not only uncommon but difficult since some SNe IIn transients can last for many decades before fading away.

1.3 Runaway Stars

Runaway stars are defined as stars that have space velocities of 30 to 40 km s^{-1} (Blaauw, 1961; Eldridge et al., 2011), though some can reach velocities over 200 km s^{-1} . As described in Eldridge et al. (2011), the two main scenarios to create runaway stars are through a dynamical ejection scenario (DES) and through a binary supernova scenario (BSS), though the fastest runaway stars could have been created by a combination of both. In the DES, stars would be ejected via encounters with other massive stars in a dense cluster - this can be single stars or even entire binary systems of stars. The BSS, on the other hand, occurs when one of the stars in a binary explodes, unbinding the system and kicking the secondary star. The two methods are expected to contribute roughly equal amounts of runaway stars, but it is possible to differentiate between the two by looking at their compositions as BSS runaways should show evidence of binary interaction (Eldridge et al., 2011). Again, since entire binary systems can be ejected in DES, it is reasonable to assume that some of those binary systems undergo BSS as well.

The most common type of runaway star are O- and B-type stars (Blaauw, 1961), massive stars that can lead to core collapse explosions. Since these stars are launched in excess of 30 km s^{-1} , it is not unreasonable that secondary stars kicked in a BSS could travel many parsecs before exploding in their own SN. The simulations run by Eldridge et al. (2011) (seen in Fig. 1.3) do in fact find that for Type II SNe as well as Type Ib and Ic SNe that these progenitors can be launched in excess of 100 pc before explosion from the star-forming region they were born in.

1.3.1 LBV Runaways as Possible SNe IIn Progenitors

While the simulations by Eldridge et al. (2011) do not look at SNe IIn specifically, Habergham et al. (2014) analyzed 39 SNe IIn and SN imposters and looking to see how they trace Hα emission (a tracer of star formation) in their host galaxies. Based on these observations, Habergham et al. (2014) concluded that not only do SNe IIn not correlate to star formation regions, they correlate even less to star formation than other explosions such as SNe II-P. The authors attribute this as an indication that SNe IIn are unlikely to have high mass progenitors, as they expect them to follow star forming regions as well as SN Ic, which have massive progenitors as well. This implies that whatever progenitor is creating many Type IIn explosions must either be low enough mass to survive longer than higher mass stars, or they have been isolated by some other means.

Although this appears to be contradictory, observations by Smith and Tombleson (2015) of LBVs in the Milky Way (MW), Large Magellanic Cloud (LMC), and Small Magallanic Cloud (SMC) imply that LBV stars almost always find themselves isolated from other O-type stars and star-forming regions (Smith and Tombleson, 2015). This matches up nicely with the view of LBVs serving as the progenitors for SNe IIn.

Smith and Tombleson (2015) analyzed 29 LBVs and LBV candidates in the MW, LMC, and SMC, and determined the distance between the object and the nearest O-type star. A plot of the cumulative fraction versus distance to nearest O-type star of several different classes of stars (Fig. 1.4) appears to show that the LBV population have a distinct distribution independent of O-type stars (which they would follow if they were all young massive stars) and RSGs (which they would follow if they are much older than expected).

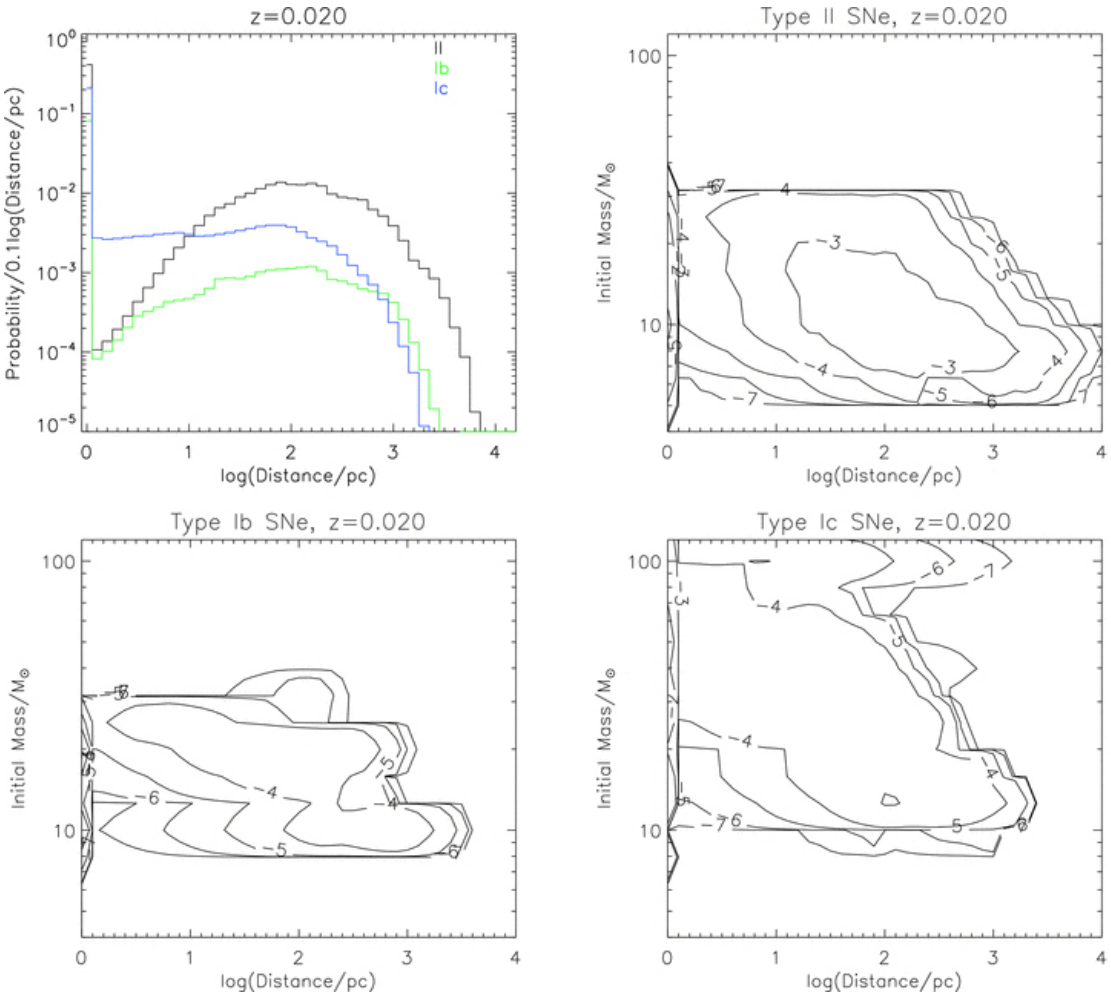

Figure 1.3: Plot showing the distribution of distance traveled by SN progenitors versus the progenitor's original mass, in solar metallicity. The data comes from the simulations of Eldridge et al. (2011). The contours represent the probability in $\log_{10}$ of a SN progenitor of that initial mass traveling that distance. This figure is from Eldridge et al. (2011).

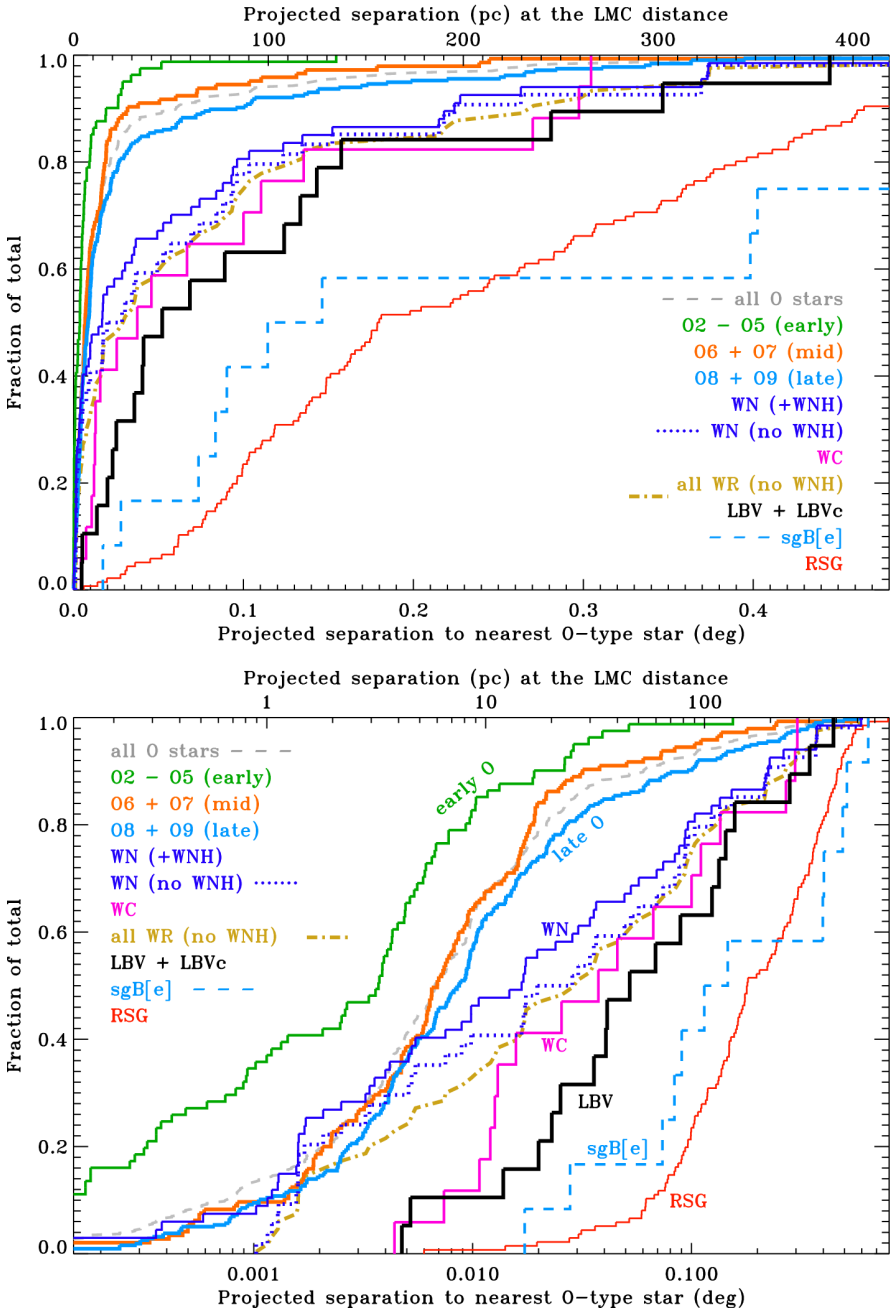

Figure 1.4: Plot comparing the cumulative fractions of different classes of stars and their distances to the nearest O-type star. The full list of classes can be seen in Fig. 4 of Smith and Tombleson (2015). All LBVs and LBV candidates from the MW, LMC, and SMC are combined into one group and appear to show that they are a distinct population from O-type stars and RSGs. This figure is from Smith and Tombleson (2015).

In order to reconcile the fact that according to traditional stellar evolution models LBVs should not be found isolated, Smith and Tombleson (2015) suggest that most LBV stars are actually the end stage for the kicked mass gaining companion in the BSS. With the LBV progenitor being kicked from its binary, Smith and Tombleson (2015) claim it can then travel the adequate distance to be found later in a region of relative isolation from other O-type stars and star forming regions. The important aspect of this scenario is that the LBV progenitor, serving as the secondary star, accretes mass through RLOF from the primary star prior to the primary star's explosion. This allows the star to substantially increase its own mass and luminosity, and therefore appear younger than the stars around it (known as "blue stragglers") (Smith and Tombleson, 2015). These stars will still have an extended lifetime compared to stars of their new mass and luminosity, and as such can travel great distances before evolving and exploding (Smith and Tombleson, 2015). Additionally, the process of RLOF will allow them to gain significant angular momentum, which may be important to LBV instabilities and eruptions (Smith and Tombleson, 2015). The velocity of the ejected star would have a direct relation to the amount of mass gained through RLOF, as stars that gain more mass would be kicked at a slower speed than a star that gained less mass.

A closer look at this from Humphreys et al. (2016) appears to directly rebutt this claim, however, and even claim that the data from Smith and Tombleson (2015) support the traditional view of LBV evolution. They achieve this by emphasizing the theorized class split of LBVs into the "classical" more luminous LBVs and the less luminous LBVs, and the important evolutionary differences between them. Because the less luminous LBVs originate from stars that have already been through a RSG phase, they should be expected to be much older than their classical counterparts and therefore have similar isolation rates to RSGs. The classical LBVs are much younger when they reach their LBV phase, and therefore should have similar isolation statistics to O-type stars. Although they have a very small sample size due to only using LMC and SMC confirmed LBVs, Humphreys et al. (2016) find this trend to be supported by the data (see Fig. 1.5).

Humphreys et al. (2016) also claim that many of the objects used by Smith and Tombleson (2015) are not truly LBVs, finding that eight of the 39 objects (six in the LMC and two in the SMC) used in the original analysis are not confirmed LBVs in the

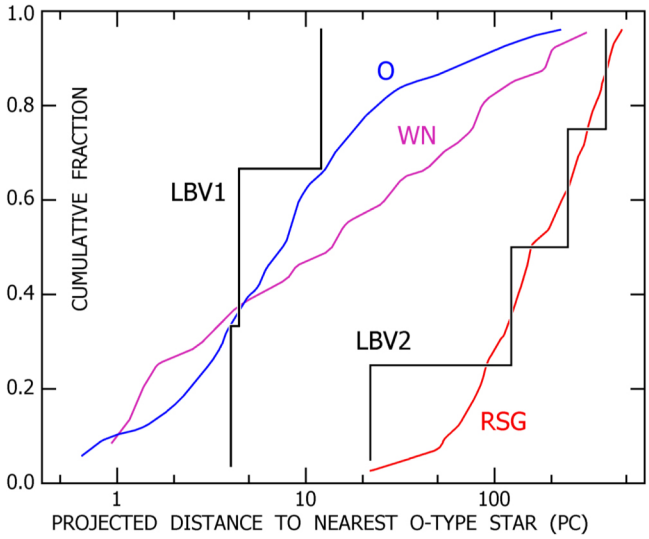

Figure 1.5: Plot comparing the cumulative fractions of different classes of stars and their distances to the nearest O-type star. Displayed are O-type stars, Wolf-Rayet WN stars, RSGs, as well as "classical" LBVs (LBV1) and less-luminous LBVs (LBV2). It is clearly shown that the classical LBVs follow O-type stars and the less luminous LBVs follow RSGs, as expected. This figure is from Humphreys et al. (2016).

literature. They are also careful to distinguish between confirmed LBVs and "candidate" LBVs, and even find that the candidates follow the same trend as RSGs as well.

Humphreys et al. (2016) finally claim that they don't find any evidence of runaway-like behavior in any of the LBVs studied. When comparing LBV velocity to the expected galactic rotational velocities at that location, they find that all but one (S119 in the LMC, with an offset velocity of over 100 km s^{-1}) have offset velocities $\leq$ 100 km s^{-1} , which they set as their minimum cut-off for a runaway star. If we take the 30 km s^{-1} prescribed by Blaauw (1961), we find that six of the 26 total LBVs and LBV candidates analyzed by Humphreys et al. (2016) may be a runaway candidate.

More notably, a runaway star is expected to have a bow shock nebula (**?**), something not commonly seen in LBVs within the MW or LMC. While we cannot clearly resolve LBVs in other galaxies, their lack of presence in our galactic neighborhood (outside of S119) casts further doubt on the possible runaway nature of LBVs.

1.4 This thesis

The goal of this thesis is to determine if we see evidence of SNe IIn arising from runaway stars, and if so, place constraints on them in the hope of learning more about their progenitors. In order to do this, I will be analyzing the narrow Hα lines of SNe IIn and comparing their line of sight velocities to the expected radial velocity of the galaxy in that location.

Chapter 2 will detail the observed supernovae I use in this thesis, as well as how they were obtained. Chapter 3 will talk about the methods used to analyze the offset velocities of the SNe IIn relative to their host galaxies. Chapter 4 will detail the findings of this thesis as well as any future work that can be done from here. Finally, Chapter 5 will conclude the findings of this thesis.

Chapter 2

Observations

2.1 Observed SNe IIn

All observations used for this thesis were taken with the DEIMOS (DEep Imaging Multi-Object Spectrograph) multi-object spectrograph on the Keck II (10-m) telescope (Faber et al., 2003). In order to collect as many SNe IIn as possible, a list of SNe IIn was obtained using the Asiago Supernova Catalog (Barbon et al., 1999), a catalog of supernovae dating from 1885 to 2017, as well as the Transient Name Server[1] from the International Astronomical Union. These were then searched in the Keck Observatory Archive to see if any observations were taken of the SNe with DEIMOS. Upon analysis, we also removed any SNe IIn that had already evolved to the point where the SN ejecta was freely expanding (there were no more narrow- or intermediate-width Hα lines). All observations used in this thesis are listed in Table 2.1. *Of note: many more SN were downloaded than were analyzed due to difficulties with the DEIMOS pipeline.*

2.2 DEIMOS

DEIMOS is a multi-object spectrograph capable of taking spectra of multiple objects at once. The slitmasks span 16.7' of the sky, and have a wavelength range of 4100 Å to 1.1 μm (Faber et al., 2003). The observations used in this thesis all utilize the Long Variable Mutlislit (LVM) slitmask. All observations taken prior to 2008 utilized four

[1] `https://wis-tns.weizmann.ac.il/`

SN	Date (UT)	Galaxy Host	Grating Used	PI
SN 2013dz	2013 Aug 2	Unknown	1200G	Filippenko, A.
SN 2013W	2013 Apr 8	UGC 5448	600ZD	Filippenko, A.
SN 2012ab	2012 Nov 15	Unknown	600ZD	Filippenko, A.
SN 2008en	2012 Sep 23	UGC 564	1200G	Filippenko, A.
SN 2010jl	2010 Nov 7	UGC 5189A	600ZD	Filippenko, A.
SN 2005R	2005 Feb 11	UGC 6274	600ZD	Davis, M.

Table 2.1: Table of observations

slitlets on the original LVM, while future ones use the LVMslitB or LVMslitC which have 5 slitlets.

DEIMOS has two separate gratings: a lower-resolution aluminized grating with 600 lines mm^{-1} (600ZD) blazed at 7500 Å which offers a width of 5300 Å; and a higher-resolution gold-coated grating with 1200 lines mm^{-1} (1200G) blazed at 7500 Å offering a width of 2630 Å.

Fig. 2.1 shows an image of SN 2010jl prior to being reduced in the DEIMOS pipeline. This image is transposed and rotated such that the x axis represents wavelength (increasing to the right) and the y axis represents the location of the emission. Several night-sky emission lines from the atmosphere can be seen in this image, and are removed in the pipeline.

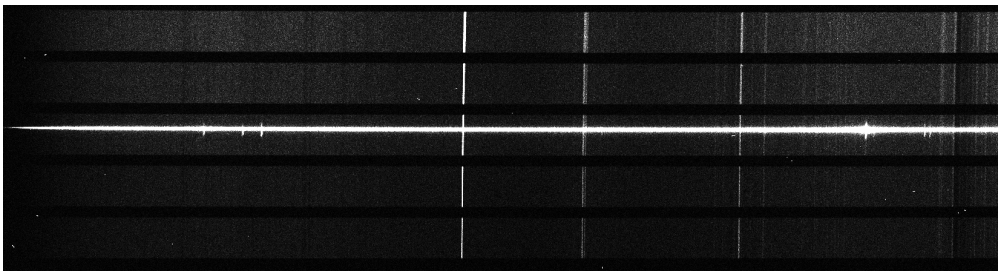

Figure 2.1: An image taken of the blue portion SN 2010jl on DEIMOS, prior to being reduced. This image is transposed and rotated such that the x axis represents wavelength (increasing to the right) and the y axis represents location in the CCD. The SN continuum is clearly visible in the middle slit, though there are some skylines still present. This image was taken as part of the Improving the Utility of Type Ia Supernovae as Probes of Dark Energy program.

2.3 Hα λ6563

Hα is the primary Balmer line of hydrogen, occurring when a hydrogen electron moves from the third energy level to the second energy level. As mentioned in Chapter 1, we expect to see strong emissions of Hα in spectra of SNe IIn due to the shock heating of the CDS. We additionally would expect to see nebular Hα tracing the SN host galaxy, as it traces high mass stars and star formation rates (as mentioned in Habergham et al. (2014)). An example Hα spectrum from a SNe IIn can be seen in Fig. 2.2 which displays the narrow (and the beginnings of intermediate) width Hα emission in SN 2008en.

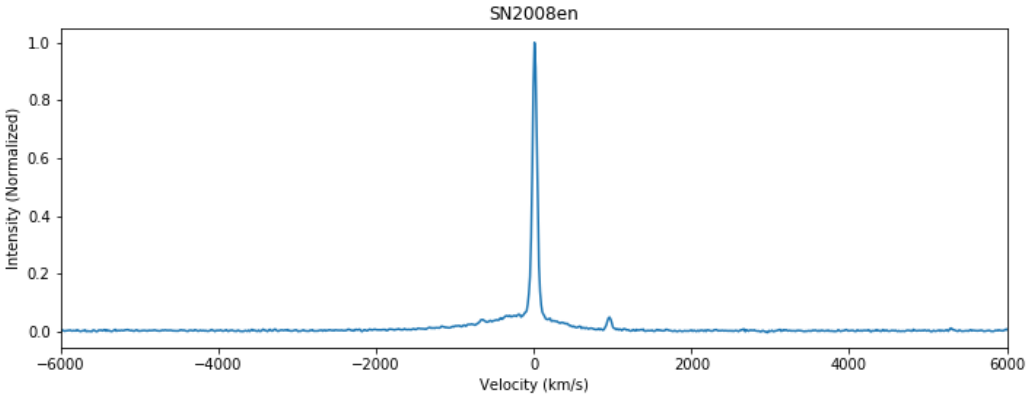

Figure 2.2: Spectrum of the Hα emission from SN 2008en. We can see here strong narrow emission lines of Hα which is flanked by weak [N II] emission on both sides. This image is centered on the narrow Hα emission and shows Doppler velocity on the x axis and normalized flux per unit wavelength on the y axis.

Since DEIMOS has a spatially extended slit, we can expect to see the SN continuum, the SN Hα, and the host galaxy Hα in the same image. An example of this can be seen in Fig. 2.3, which displays the Hα of SN 2013dz and its host galaxy. What is typically seen in these observations is a bright continnuum emission from the SN, making it difficult to visiually distinguish the Hα emission. We also see Hα emission that traces the host galaxy's emission.

One property of this image that is easy to notice is that the galactic Hα shifts from left to right in wavelength. This is expected, as this shift represents the Doppler shift of different parts of the galaxy. In Fig. 2.3, the bottom portion of the galaxy is blueshifted, indicating its line of sight velocity is pointed towards the observer, while the top portion

is redshifted. This shift can be used to estimate what radial velocity is expected of the SN IIn if it were not a runaway star.

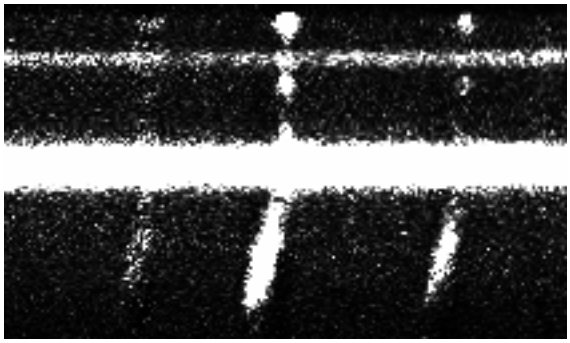

Figure 2.3: An image taken of the red portion of SN 2013dz on DEIMOS, after being reduced. We can clearly see the Hα emission from the host galaxy as well as the continuum emission of SN 2013dz. We also can see N II λ6548 and N II λ6583 lines of the host galaxy. The Hα emission of the SN is difficult to distinguish visually as the SN continuum is already extremely bright.

Chapter 3

Analysis

3.1 Reducing DEIMOS Images

We used the Carnegie Python Distribution (CarPy)[1] in order to handle, calibrate, reduce, and analyze the images observed from DEIMOS (Kelson et al., 2000; Kelson, 2003). CarPy includes many routines for processing multi-slit spectroscopic data. The CarPy environment also contains PyRAF[2] , a Python based command language to run IRAF[3] (Image Reduction and Analysis Facility) tasks.

Our reduction is based on the standard prescription outlined in Silverman et al. (2012), with slight modifications. Since all of the observations were made on the same instrument (DEIMOS), the only changes that need to be made between different observations is based on the placement of the slitlets, the number of slitlets, and the resolution of the gratings. I will summarize the our pipeline below:

1. Subtract out the overscan region and subtract out the bias. For this, we use `iraf.ccdproc`. Then transpose the image and rotate it 180 degrees such that wavelength is increasing in the $+x$ direction of the image.

2. Combine and normalize the flat-fields using `iraf.flatcombine`.

[1] `https://code.obs.carnegiescience.edu/carnegie-python-distribution`

[2] PyRAF is a product of the Space Telescope Science Institute, which is operated by AURA for NASA.

[3] The Image Reduction and Analysis Facility is distributed by the National Optical Astronomy Observatory, which is operated by the Association of Universities for Research in Astronomy (AURA), Inc., under cooperative agreement with the National Science Foundation (NSF)

3. Rectify the image using the combined flat-fields. The y-distortion is calculated using `getrect` and then applied to the flats using `copyrect` such that the wavelength in every vertical strip is the same.

4. Find the locations of the slitlets in the images using `findslits`. Once the slits are found, the locations are written to the image header and copied to the rest of the images.

5. Divide out the flat fields and the blaze from the other images using `flat2d`.

6. Get the rectification for each slit using `getrect`, and then copy them to all the other images using `copyrect`. In this step, we are specifically copying the x-distortion.

7. Calibrate the wavelength scale with `waverect`. This uses the assistance of arc-lamp spectra, which typically contained Neon, Argon, Krypton, and Xenon, and sometimes Cadmium, Zinc, and Mercury. This gets applied to all the images.

8. Extract the 1D spectra of the standard star using `iraf.apall`. We interactively remove telluric and absorption features using `iraf.splot` to select the regions and then dividing them out using `iraf.sarith`. This forms a standard continuum spectrum, as well as a sensitivity function.

9. Extract the 1D spectra of the SN, and normalize by the standard continuum. Apply telluric corrections using `iraf.telluric`, and flux calibrate using the sensitivity function.

10. Combine the spectra of the blue and red sides to form one complete spectrum. We can then analyze the location of the peak as well as get a full-width half-maximum (FWHM) measurement of the Hα using `splot`.

3.2 Analyzing Velocities of SNe IIn

Once we are able to extract the spectra, we want to run steps 9 and 10 from Sec. 3.1 for different points of the galaxy's Hα line, as well as on the continuum of the SN to measure the Hα emission of the SN. In order to determine the central location and the FWHM

of the emission, we utilize a multi-component fit of Lorentzian profiles, determining the narrow-width and intermediate-width emission making up the overall profile. We can then map out the Hα emission throughout the galaxy.

With this map, we attempt to fit a fourth order polynomial function through the galaxy Hα emission. This function provides an upper estimate for the peak wavelength of the galaxy's Hα emission at the location of the supernova, and we can then determine the offset velocity of the SN using a line-of-sight velocity calculation

$$v = \frac{c\left(\lambda_{\text{gal}} - \lambda_{\text{SN}}\right)}{\lambda_{\text{gal}}} \tag{3.1}$$

where v is the offset velocity, c is the speed of light (3×10^5 km s^{-1}), λ_{gal} is the estimated wavelength of Hα emission of the galaxy at the SN location, and λ_{SN} is the observed wavelength of the SN Hα emission.

Our results for all observed galaxies can be seen in Table 3.2. The spectra of all the SNe can be seen in Fig. 3.1 and Fig. 3.2. Comparisons of the SNe Hα peak to the host galaxy's estimated Hα peak can be seen in Sec. B.

As mentioned in Sec. 1.1.1, after their explosion SNe IIn can be seen with a narrow-width Hα emission that represents electron-scattering in the unshocked CSM and photosphere, as well as an intermediate-width Hα emission the results from the reheating of the CDS by the shock. Those with more prominent intermediate-width lines can be assumed to have exploded further in the past from the observation compared to those with less prominent intermediate-width lines. As we can see, it appears that SN 2008en and SN 2013dz were caught relatively close to explosion, while the others (especially SN 2012ab) were caught weeks or months after explosion.

3.2.1 Limitations and Uncertainties

In order to calculate uncertainties for the offset velocities of the SNe, we utilize a jackknife re-sampling of the host galaxy's spectra (when possible). We find uncertainties in the calculated offset velocities of nearly 30 km s^{-1} in SN 2013dz and SN 2005R, and smaller uncertainties in SN 2010jl and SN 2008en. The size of these uncertainties can be tied directly to how well the generated polynomial function fit the data, as SN 2013dz

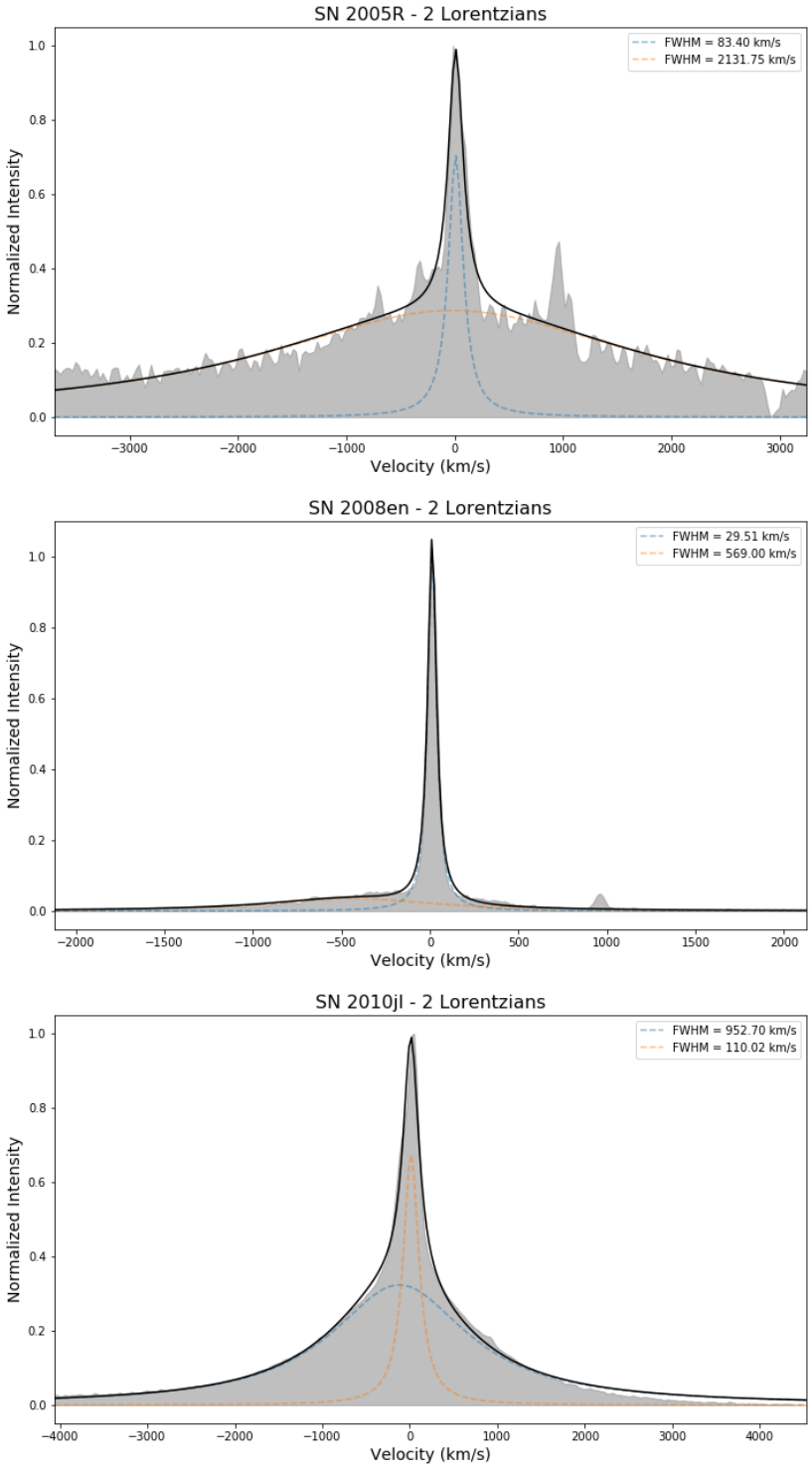

Figure 3.1: Lorentzian fits of three analyzed SNe IIn - SN 2005R, SN 2008en, and SN 2010jl. These are fit with an intermediate-width and narrow-width Lorentzian.

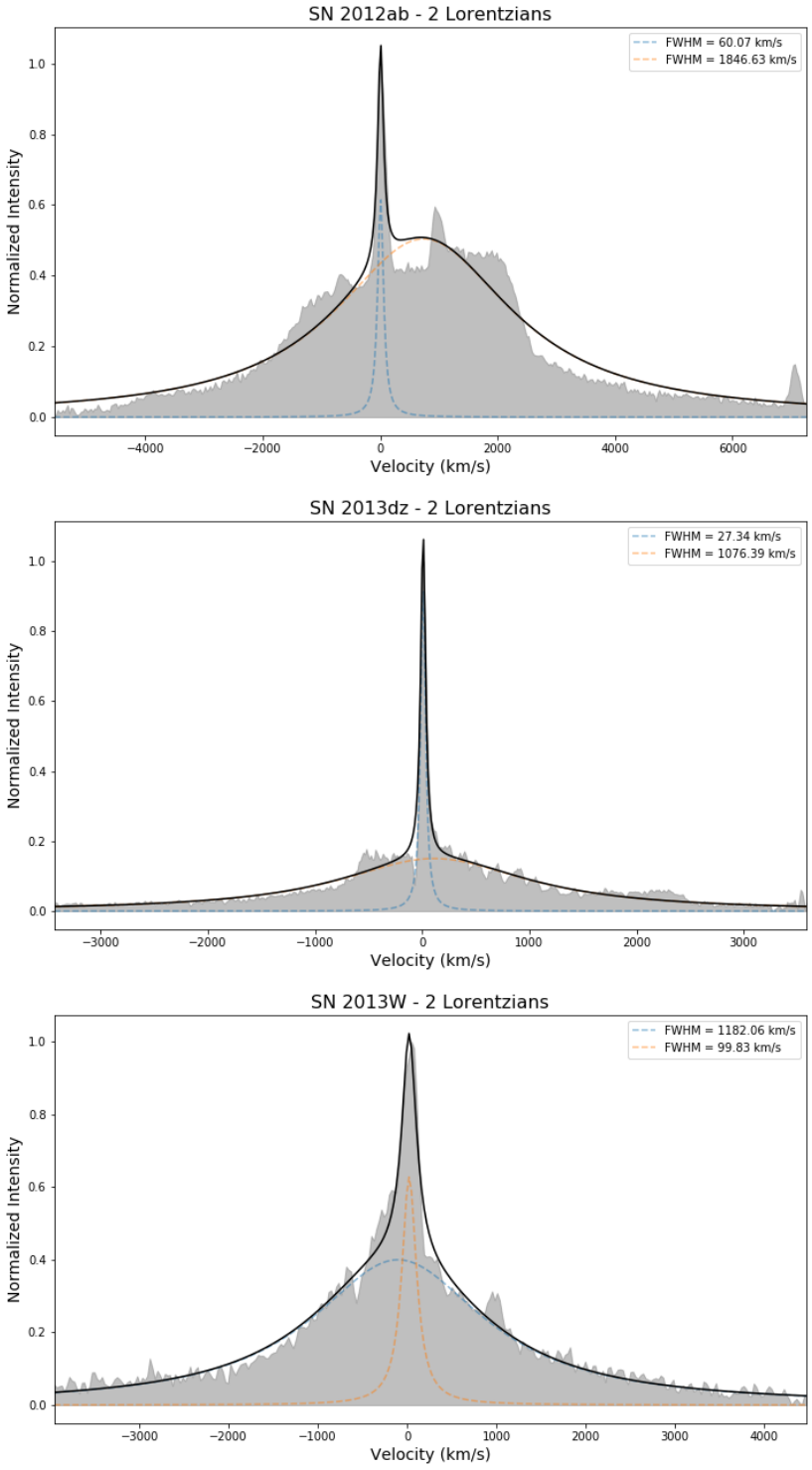

Figure 3.2: Lorentzian fits of three analyzed SNe IIn - SN 2012ab, SN 2013dz, and SN 2013W. These are fit with an intermediate-width and narrow-width Lorentzian.

SN	Offset Velocity (km s^{-1})	Narrow-width FWHM (km s^{-1})
SN 2013dz	$33.55^{+27.97}_{-13.53}$	27.34
SN 2013W	$15.64^{\dagger}$	99.83
SN 2012ab	$14.51^{\dagger}$	60.07
SN 2010jl	$44.86^{+7.70}_{-12.96}$	29.51
SN 2008en	$1.66^{+0.67}_{-0.45}$	110.02
SN 2005R	$8.20^{+28.22}_{-6.71}$	83.40

Table 3.1: List of SNe IIn, the FWHM of their Hα emission, and their offset velocities from their host galaxies. Uncertainties arise from a jackknife re-sampling of host galaxy spectra. A † indicates that jackknife re-sampling was unable to be executed.

and SN 2005R have more variation off of the fit function compared to SN 2010jl and SN 2008en.

Such uncertainties may have arisen from the choosing of points in the host galaxy to analyze, as some locations within the host galaxy may be contaminated by other Hα sources that are themselves moving relative to the host galaxy. Additionally, the resolution of points sampled from the host galaxy can limit the accuracy of the fit. Sampling more points from the host galaxy would allow us to determine a more accurate shape of the galaxy's line of sight velocity and therefore more accurately determine the offset velocity of the SN.

In order to truly know the offset velocity of the SN analyzed, new observations can be taken of the host galaxy after the SN has faded for runaway candidates. The wavelength of the Hα peak of the host galaxy at the location of the SN could then be taken, and a more accurate offset velocity then calculated.

Chapter 4

Discussion

Recalling back to Sec. 1.3, Eldridge et al. (2011) and Blaauw (1961) define runaway stars to have space velocities above 30 to 40 km s^{-1} . If we look at Table 3.2, we only see two objects that fulfill this definition - SN 2013dz with an offset velocity of $33.55^{+27.97}_{-13.53}$ km s^{-1} and SN 2010jl with an offset velocity of $44.86^{+7.70}_{-12.96}$ km s^{-1} . All of the other SN have velocities below 20 km s^{-1} within uncertainties. It is worth noting that none of these SNe fulfill the definition set by Humphreys et al. (2016) of 100 km s^{-1} .

This data, and more significantly the amount of data we analyzed, makes it extremely difficult to come to any significant conclusions. Having only six data points to work with means that it is unreasonable and irresponsible to claim that many SNe IIn arise from runaway LBVs - but the presence of SN 2013dz and SN 2010jl as possible candidates does give it credence.

4.1 Runaway Candidates

In this paper, we will define runaway candidates as having a space velocity greater than 30 km s^{-1} .

4.1.1 SN 2010jl

With a space velocity of $44.86^{+7.70}_{-12.96}$ km s^{-1} with respect to its host galaxy local environment, we claim that SN 2010jl is a candidate to have a runaway progenitor. As can

be seen in Fig. 4.1, there is a significant shift towards the red in the peak Hα wavelength of the SN with respect to the host galaxy at the SN position along the slit.

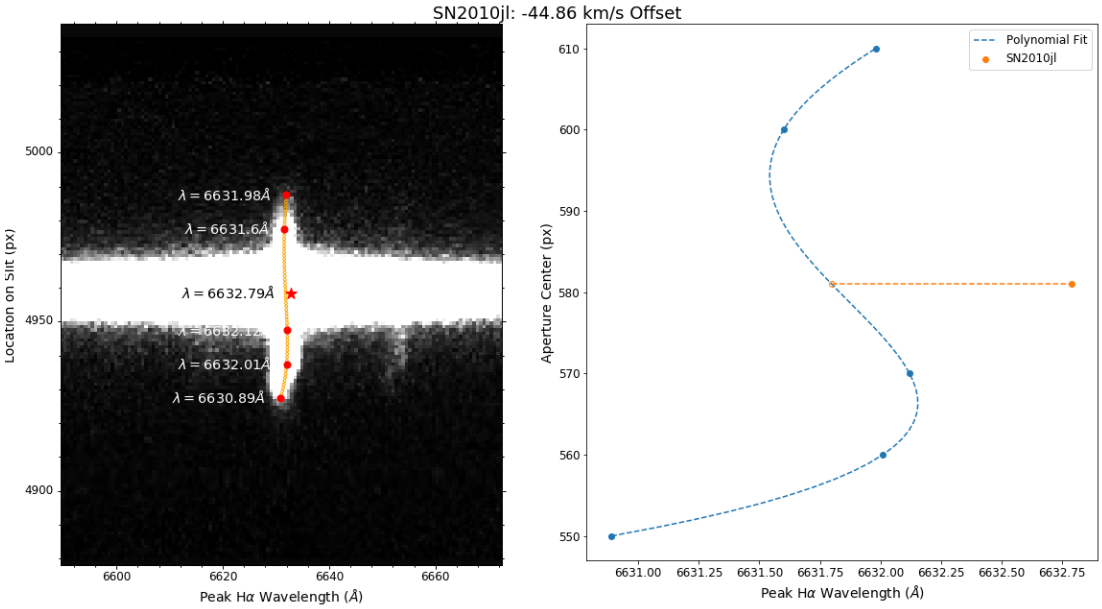

Figure 4.1: SN 2010jl Hα relative to host galaxy. A clear displacement of the Hα peak of the SN can be seen relative to the host galaxy, implying that the progenitor may have been a runaway. *Left panel:* Slit image of SN 2010jl taken by DEIMOS, with red circles marking the location of the Hα peak in the host galaxy. The orange dots represent the cubic polynomial fit to the host galaxy Hα . The red star represents the location of the Hα peak of the SN. *Right panel:* Zoomed in view of the host galaxy and SN Hα peaks. The blue dots represent the location of the Hα peak in the host galaxy, with the blue dashed line representing the cubic polynomial fit. The orange closed dot represents the location of the SN Hα peak while the orange open dot represents represents where it would be if not offset. The orange dotted line shows the offset.

Smith et al. (2011) goes into detail about the progenitor star of SN 2010jl, as it is one of a few SNe IIn with direct observations of the progenitor prior to explosion. Hubble Space Telescope (HST) observations of the progenitor about 10 years prior to explosion show a luminous and blue point source at the location of the SN, implying that the progenitor could have been in a massive young star cluster or a LBV.

However, it is hard to reconcile the predicted initial mass of 80 $M_{\odot}$ with a runaway. If it were a runaway companion star, it would fall on the higher end of expected masses

in Smith and Tombleson (2015) as a star with $M_{\mathrm{ZAMS}} \approx 30 - 40 M_{\odot}$ accreting enough mass to appear as a $60 - 80 M_{\odot}$ star. It is certainly not unreasonable to claim that the predicted progenitor mass, the observed offset velocity, and visual observations of the progenitor could imply a runaway LBV progenitor, but it is pushing at the lower limits of runaway stars and the higher limits of mass-gaining RLOF stars. Additionally, such a massive star might have difficulty even reaching a runaway velocity when kicked through BSS.

If we consider the traditional view of LBVs, an $80 M_{\odot}$ LBV would almost certainly be a classical-type LBV. Because of this, we would expect it to have undergone further evolution into a WN star and then a WC star before explosion, but in order for the CSM to be dense enough to emit narrow lines, this period must have been short as hypothesized by Dwarkadas (2011).

Smith et al. (2011) also theorize that the progenitor star could have been a normally fainter and less massive LBV that just happened to be caught by HST mid-eruption. Since such an eruption can last on the order of 10 years, they claim this situation is not improbable. The supernova explosion would then have to happen soon after the LBV eruption or even during it - a situation possibly paralleled by SN 2009ip (Mauerhan et al., 2012). Since the progenitor star would not have to be as massive as $80 M_{\odot}$, it is much more reasonable to believe that it can reach speeds over 40 km s^{-1} when ejected through BSS.

The last possible progenitor type presented by Smith et al. (2011) resided in an extremely massive star cluster with an age around 5 Myr. This would present a progenitor star with $M_{\mathrm{ZAMS}} > 30 M_{\odot}$. Such a star could have been ejected through DES, providing it with it's higher space velocity, but it does not explain how the progenitor gained the dense CSM necessary to explode as a SN IIn. If it fell within the traditional view of LBVs, it could possibly be an extremely massive classical LBV that quickly evolved to its SN stage, ejected via DES.

4.1.2 SN 2013dz

SN 2013dz has a space velocity of $33.55^{+27.97}_{-13.53}$ km s^{-1} with respect to its host galaxy local environment, and as such we claim it is a candidate to have a runaway progenitor. Here we see a shift to the red in the peak Hα wavelength of the SN. The polynomial fit

is not entirely in line with the host galaxy Hα peaks, but the offsets of the host galaxy peaks are much smaller than that of the SN.

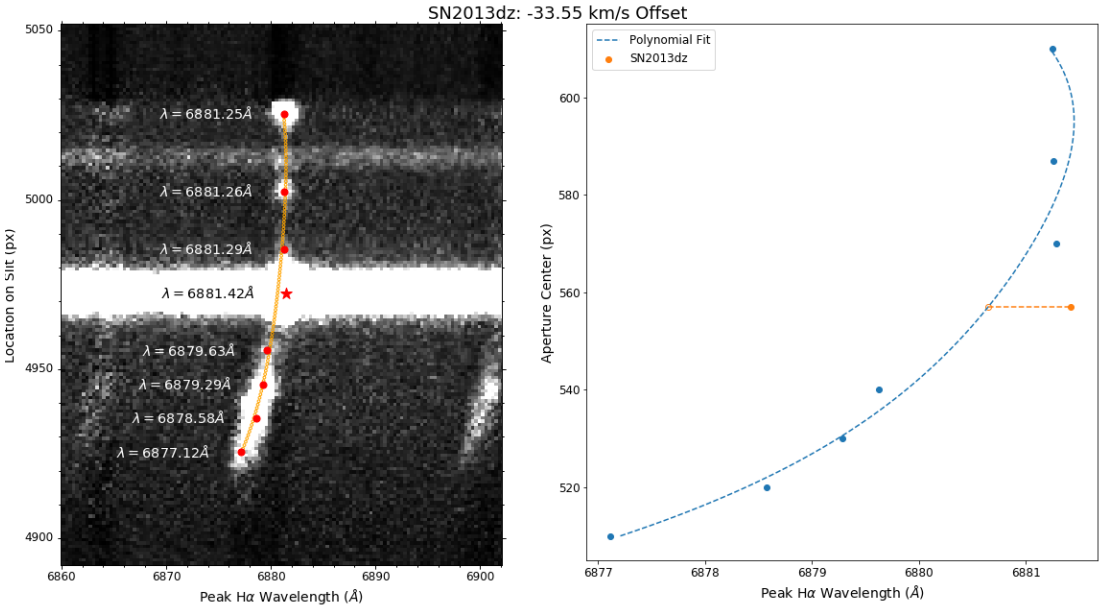

Figure 4.2: SN 2013dz Hα relative to host galaxy. While the offset between the SN and host galaxy is not as drastic as it is for SN 2010jl, the SN Hα peak is clearly seperate from the host galaxy. Keys to both panels can be seen in Fig. 4.1.

Unlike SN 2010jl, there are no analyses of SN 2013dz in scientific literature. It was discovered by Dhungana et al. (2013) in July 2013 and observed again 20 days later using DEIMOS. The one dimensional spectrum from DEIMOS can be seen in Fig. 3.2. In it, there is blue-shifted hydrogen component and P-Cygni absorption that bears strong similarities to the blue-shifted components of SN 2013L, especially in early times (Andrews et al., 2017, see their Fig. 8, 9). Andrews et al. (2017) claim that this suggests that the SN ejecta began interacting with very dense CSM at this time (approximately 30 d after explosion). If we take the date of first observation by Dhungana et al. (2013) as approximately 10 d after explosion, this timeline matches up exactly with SN 2013L.

Andrews et al. (2017) further analyze the evolution of the spectrum of SN 2013L and come to the conclusion that the progenitor star must have had extremely asymmetric CSM in order to generate the Hα profile, suggesting an initial mass of $M > 25M_{\odot}$. They also suggest that the asymmetry could be a result of binary RLOF, however it is

believed to be in the shape of a torus or disc and not a bow shock. Andrews et al. (2017) also derive a mass-loss rate for the progenitor of SN 2013L being between 1×10^{-4} and $1 \times 10^{-3} M_{\odot}$ yr^{-1}, implying a yellow hypergiant or quiescent LBV.

While we clearly cannot take their results and apply it to SN 2013dz, the similarities in the Hα profile do lend their hand to SN 2013dz's progenitor being some sort of massive star with a very asymmetric CSM. It can be implied that, while not the result of an eruptive LBV, the progenitor could have been ejected through BSS after gaining significant mass and CSM through RLOF.

We should also account for the large range of uncertainties in the measured offset velocity. At its very highest end, the progenitor star may have been traveling at over 60 km s^{-1} relative to its local environment (a clear candidate to have a runaway progenitor star), while at its lowest end it may have only been traveling at 20 km s^{-1} (below the 30 km s^{-1} definition of a runaway star). While much of this uncertainty stems from the variance of host galaxy Hα emission off the polynomial fit, it further emphasizes the need for follow up observations of the host galaxy.

4.2 Implications on progenitors

Having two candidates for runaway progenitors is scientifically interesting, despite having a small sample size. It would be fair to claim that projection effects may be at play with some of the other SNe IIn in our sample, as if they were ejected, their motion may not be directly towards or away from the observer. A lack of observed Doppler velocity difference may be a result of the progenitor not being ejected through BSS or DES, or it could be the result of the progentior simply being ejected in a direction that we cannot discern a velocity through Doppler shift. The lack of any SN having an offset over 45 km s^{-1} , nevertheless up to 100 km s^{-1} as Humphreys et al. (2016) demar does imply that having a runaway progenitor is unlikely.

Even if projection effects are accounted for, the lack of possible runaway progenitors is worth discussion. If, as many claim, LBV stars serve as the typical progenitor for SNe IIn, then we could possibly assume that the progenitors of these SNe without high velocities are more massive classical LBVs who explode before they can be travel far (matching Humphreys et al. (2016)), or that they gained so much mass in RLOF that

they simply could not be kicked at sufficient enough velocity to be classified as a runaway candidate. If most LBVs are truly runaway stars, then the lack of candidate runaway progenitors for SNe IIn could imply that LBVs are not the typical progenitor star for SNe IIn. This would require more creative solutions to the SNe IIn in the literature with LBV progenitors, or recognition that the observed SNe IIn are atypical for their class.

With that being said, it is important to recall that SNe IIn are *external phenomena* and do not necessarily arise from a single type of progenitor. Any astrophysical event that leads to significant CSM surrounding a progenitor can lead to a SN IIn event, and as such we should not expect every SN IIn to arise from a runaway star, let alone a runaway LBV as Smith and Tombleson (2015) implies.

Chapter 5

Conclusion

After spectral analysis of six Type IIn supernovae observed with DEIMOS, we find two candidate runaway progenitors (for SN 2013dz and SN 2010jl) with offset velocities of 30 km s^{-1} or greater relative to their location in their host galaxy. This offset velocity implies that the progenitors of these explosions may have undergone some sort of ejection, either through dynamical interaction with star clusters or through the death of its binary pair. This raises the possibility that, at the very least, some SNe IIn progenitors may be the result of runaway stars. SN 2010jl in particular is the closest thing to a confirmed runaway LBV progenitor for the resulting SNe IIn, having been observed by Hubble approximately 10 years prior to explosion. SN 2013dz, while not present in the literature, shows signs of having an asymmetric CSM which could be caused by bipolar LBV eruptions, binary RLOF, or both.

The remaining four supernovae analyzed, however, show little to no significant offset velocity. This could be the result of two separate scenarios: (1) the progenitors of these SNe IIn gained so much mass that it did not receive a significant kick at the time of explosion or (2) the progenitors were fast-evolving "classical" LBVs, exploding after progressing to a WN stage before it can be ejected through DES or BSS. Learning more about the progenitor stars of SNe IIn would be required in order to determine which of these two is more likely.

The presence of both possible candidate runaway progenitors and non-runaway progenitors could imply a "happy medium", where some may be caused by runaway stars and others are caused by extremely massive, fast-burning stars. After all, SNe IIn are

external phenomena, and as such the dense CSM seen in them could mask a variety of other SNe types, each with their own set of progenitors.

5.1 Future Work

The limitations in methodology and small sample size of SNe IIn prohibit us from making any significant conclusions about SNe IIn as a whole. Our methods have large uncertainties surrounding them due to the estimations made as well as possible contamination of the images, and any uncaught errors in the reduction pipeline may exacerbate these. In order to obtain a more accurate measurement of the host galaxy's Hα peak at the SN location, follow up observations can be taken to measure the emission fo the galaxy itself. This would require the SN to have faded (which in some cases may take many years), but would be the best method of reducing the uncertainty in offset velocity. This would also help us determine if these events were truly SNe or not, as some of them may actually be SN imposters.

Work can still be done on getting the pipeline to work on the remaining SNe IIn observed by DEIMOS as well, that way a more significant population of SNe IIn can be analyzed. Additionally, increases in all-sky surveys can help future astrophysicists pinpoint possible progenitors for future explosions, much like what was done for SN 2010jl. Getting pre-explosion direct observations is quite rare, and increasing the number of such observations can help future studies more accurately describe the immediate progenitors of these explosions. Timely notifications of new transients can also help identify SNe IIn prior to their intermediate-width lines taking over the spectrum, and will help get actionable data.

Ultimately, it is too soon to tell if a large proportion of SNe IIn are caused by runaway stars, and more research (both with observations and with evolutionary models) is needed to determine if there truly is a relationship.

References

Jennifer E. Andrews, Nathan Smith, Curtis McCully, Ori D. Fox, S. Valenti, and D. A. Howell. Optical and IR observations of SN 2013L, a Type IIn Supernova surrounded by asymmetric CSM. *Monthly Notices of the Royal Astronomical Society*, 471(4): 4047–4059, 7 2017. ISSN 13652966. doi: 10.1093/MNRAS/STX1844.

R. Barbon, V. Buondí, E. Cappellaro, and M. Turatto. The Asiago Supernova Catalogue - 10 years after. *Astronomy and Astrophysics Supplement Series*, 139(3):531–536, 11 1999. ISSN 03650138. doi: 10.1051/aas:1999404.

A. Blaauw. On the origin of the O and B-type stars with high velocities. *Bulletin of the Astronomical Institutes of the Netherlands*, 15:265, 1961. ISSN 0004-6361.

G. Dhungana, J. M. Silverman, W. Zheng, R. Kehoe, F. V. Ferrante, J. Vinko, G. H. Marion, R. Quimby, F. Yuan, J. C. Wheeler, and C. Akerlof. Supernova 2013dz. *CBET*, 3589:1, 2013.

V. Dwarkadas. On luminous blue variables as the progenitors of core-collapse supernovae, especially Type IIn supernovae. *Monthly Notices of the Royal Astronomical Society*, 412(3):1639–1649, 4 2011. ISSN 00358711. doi: 10.1111/j.1365-2966.2010.18001.x.

John J. Eldridge, Norbert Langer, and Christopher A. Tout. Runaway stars as progenitors of supernovae and gamma-ray bursts. *Monthly Notices of the Royal Astronomical Society*, 414(4):3501–3520, 3 2011. ISSN 00358711. doi: 10.1111/j.1365-2966.2011.18650.x.

Sandra M. Faber, Andrew C. Phillips, Robert I. Kibrick, Barry Alcott, Steven L. Allen,

Jim Burrous, T. Cantrall, De Clarke, Alison L. Coil, David J. Cowley, Marc Davis, William T. S. Deich, Ken Dietsch, David K. Gilmore, Carol A. Harper, David F. Hilyard, Jeffrey P. Lewis, Molly McVeigh, Jeffrey Newman, Jack Osborne, Ricardo Schiavon, Richard J. Stover, Dean Tucker, Vernon Wallace, Mingzhi Wei, Gregory Wirth, and Christopher A. Wright. The DEIMOS spectrograph for the Keck II Telescope: integration and testing. In Masanori Iye and Alan F. M. Moorwood, editors, *Instrument Design and Performance for Optical/Infrared Ground-based Telescopes*, volume 4841, page 1657. SPIE, 3 2003. doi: 10.1117/12.460346.

G. Gräfener and W. R. Hamann. Mass loss from late-type WN stars and its Z-dependence: Very massive stars approaching the Eddington limit. *Astronomy and Astrophysics*, 482(3):945–960, 5 2008. ISSN 00046361. doi: 10.1051/0004-6361:20066176.

S. M. Habergham, J. P. Anderson, P. A. James, and J. D. Lyman. Environments of interacting transients: Impostors and Type IIn supernovae. *Monthly Notices of the Royal Astronomical Society*, 441(3):2230–2252, 4 2014. ISSN 13652966. doi: 10.1093/mnras/stu684.

Roberta M. Humphreys and Kris Davidson. The luminous blue variables: Astrophysical geysers. *Publications of the Astronomical Society of the Pacific*, 106:1025, 10 1994. ISSN 0004-6280. doi: 10.1086/133478.

Roberta M. Humphreys, Kerstin Weis, Kris Davidson, and Michael S. Gordon. ON THE SOCIAL TRAITS OF LUMINOUS BLUE VARIABLES. *The Astrophysical Journal*, 825(1):64, 2016. ISSN 0004-637X. doi: 10.3847/0004-637x/825/1/64.

Daniel D. Kelson. Optimal Techniques in Two-dimensional Spectroscopy: Background Subtraction for the 21st Century. *Publications of the Astronomical Society of the Pacific*, 115(808):688–699, 6 2003. ISSN 0004-6280. doi: 10.1086/375502.

Daniel D. Kelson, Garth D. Illingworth, Pieter G. van Dokkum, and Marijn Franx. The Evolution of Early-Type Galaxies in Distant Clusters. II. Internal Kinematics of 55 Galaxies in the Cluster Cl 1358+62. *The Astrophysical Journal*, 531(1):159–183, 8 2000. ISSN 0004-637X. doi: 10.1086/308445. URL `http://arxiv.org/abs/astro-ph/9908257http://dx.doi.org/10.1086/308445`.

N. Langer, M. Lennon, and F. Najarro. Towards an understanding of very massive stars. A new evolutionary scenario relating O stars, LBVs and Wolf-Rayet stars. *ASTRONOMY AND ASTROPHYSICS -BERLIN-*, 290(3):819–819, 1994. ISSN 0004-6361.

Jon C. Mauerhan, Nathan Smith, Alexei Filippenko, Kyle Blanchard, Peter Blanchard, Chadwick F. E. Casper, S. Bradley Cenko, Kelsey I. Clubb, Daniel Cohen, Kiera Fuller, Gary Li, and Jeffrey M. Silverman. The Unprecedented 2012 Outburst of SN 2009ip: A Luminous Blue Variable Becomes a True Supernova. 9 2012. doi: 10.1093/mnras/stt009.

E. Schlegel. A new subclass of type II supernovae? *Monthly Notices of the Royal Astronomical Society*, 244(2):269–271, 1990. ISSN 0035-8711.

Jeffrey M. Silverman, Ryan J. Foley, Alexei V. Filippenko, Mohan Ganeshalingam, Aaron J. Barth, Ryan Chornock, Christopher V. Griffith, Jason J. Kong, Nicholas Lee, Douglas C. Leonard, Thomas Matheson, Emily G. Miller, Thea N. Steele, Brian J. Barris, Joshua S. Bloom, Bethany E. Cobb, Alison L. Coil, Louis Benoit Desroches, Elinor L. Gates, Luis C. Ho, Saurabh W. Jha, Michael T. Kandrashoff, Weidong Li, Kaisey S. Mandel, Maryam Modjaz, Matthew R. Moore, Robin E. Mostardi, Marina S. Papenkova, Sung Park, Daniel A. Perley, Dovi Poznanski, Cassie A. Reuter, James Scala, Franklin J.D. Serduke, Joseph C. Shields, Brandon J. Swift, John L. Tonry, Schuyler D. Van Dyk, Xiaofeng Wang, and S. Diane. Berkeley Supernova Ia Program - I. Observations, data reduction and spectroscopic sample of 582 low-redshift Type Ia supernovae. *Monthly Notices of the Royal Astronomical Society*, 425 (3):1789–1818, 9 2012. ISSN 00358711. doi: 10.1111/j.1365-2966.2012.21270.x.

Nathan Smith. Interacting Supernovae: Types IIn and Ibn. In *Handbook of Supernovae*, pages 403–429. Springer International Publishing, 12 2017. doi: 10.1007/978-3-319-21846-5{_}38.

Nathan Smith and Stanley P. Owocki. On the Role of Continuum-driven Eruptions in the Evolution of Very Massive Stars and Population III Stars. *The Astrophysical Journal*, 645(1):L45–L48, 7 2006. ISSN 0004-637X. doi: 10.1086/506523.

Nathan Smith and Ryan Tombleson. Luminous blue variables are antisocial: Their isolation implies that they are kicked mass gainers in binary evolution. *Monthly*

Notices of the Royal Astronomical Society, 447(1):598–617, 6 2015. ISSN 13652966. doi: 10.1093/mnras/stu2430.

Nathan Smith, Ryan Chornock, Weidong Li, Mohan Ganeshalingam, Jeffrey M. Silverman, Ryan J. Foley, Alexei V. Filippenko, and Aaron J. Barth. SN 2006tf: Precursor Eruptions and the Optically Thick Regime of Extremely Luminous Type IIn Supernovae. *The Astrophysical Journal*, 686(1):467–484, 10 2008. ISSN 0004-637X. doi: 10.1086/591021.

Nathan Smith, Weidong Li, Adam A. Miller, Jeffrey M. Silverman, Alexei V. Filippenko, Jean Charles Cuillandre, Michael C. Cooper, Thomas Matheson, and Schuyler D. Van Dyk. A massive progenitor of the luminous type IIn supernova 2010jl. *Astrophysical Journal*, 732(2), 11 2011. ISSN 15384357. doi: 10.1088/0004-637X/732/2/63.

Appendix A

Glossary and Acronyms

Care has been taken in this thesis to minimize the use of jargon, but this cannot always be achieved. This appendix defines jargon terms in a glossary, and contains a table of acronyms and their meaning.

A.1 Glossary

- **Binary Supernova Scenario** - A method of ejecting stars that involves a binary star system becoming unbound. This typically occurs when one of the stars explodes, kicking the secondary star with significant velocity.
- **Circumstellar medium** - Dense gas surrounding a star, usually caused by winds from the star as it ages and releases its outer envelopes. More dense CSM can be created from LBV eruptions.
- **Dynamical Ejection Scenario** - A method of ejecting stars that involves close encounters with massive stars or star clusters. Such stars could become slingshotted out of their original system at high speeds.
- **Full-width half-maximum** - The measured width of a given Gaussian/Lorentzian distribution. It is taken at the half-maximum of the distribution.
- **Light curve** - The measure of luminosity over a period of time. For supernovae, this will sharply increase at the time of explosion before dropping off gradually.

- **Luminous blue variable** - A massive evolved star that is prone to violent eruptions. These can be split into two classes based on intial mass and evolution (see Sec. 1.2).

- $M_{\odot}$ - The mass of the Sun, 1.989×10^{33} g. Many massive astronomical objects are meassured in units of solar masses.

- **Roche lobe** - The region around a star where matter orbiting is gravitationally bound. It is most relevant when applied to binary star systems, where the Roche lobes of each star meet at a single point.

- **Roche lobe overflow** - A method of mass transfer between stars in a binary system. It occurs when one star in the system expands to become so large that its surface extends past its Roche lobe and flows towards the other star in the system.

- **Zero-age main sequence mass** - The initial mass of a star.

A.2 Acronyms

Table A.1: Acronyms

Acronym	Meaning
BSS	Binary Supernova Scenario
CSM	CircumStellar Material
DEIMOS	DEep Imaging Multi-Object Spectrograph
DES	Dynamical Ejection Scenario
HST	Hubble Space Telescope
IRAF	Image Reduction and Analysis Facility
LBV	Luminous Blue Variable
LVM	Long View Mirror
RLOF	Roche Lobe OverFlow
SN	SuperNova (plural SNe, SuperNovae)
SNe IIn	SuperNova type IIn

Appendix B

Images and Spectra

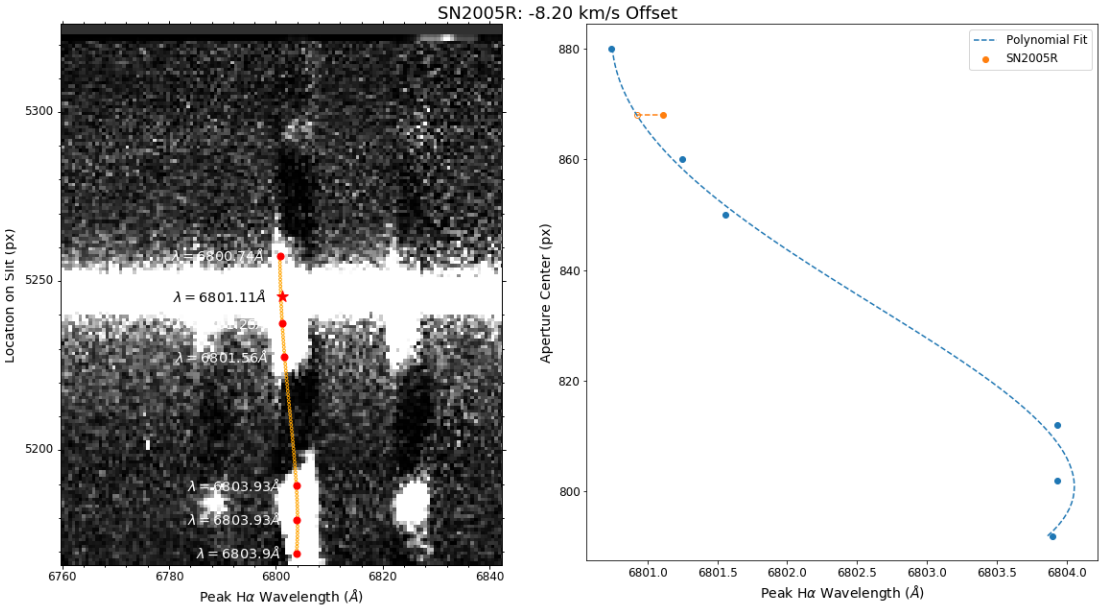

Figure B.1: SN 2005R Hα relative to host galaxy

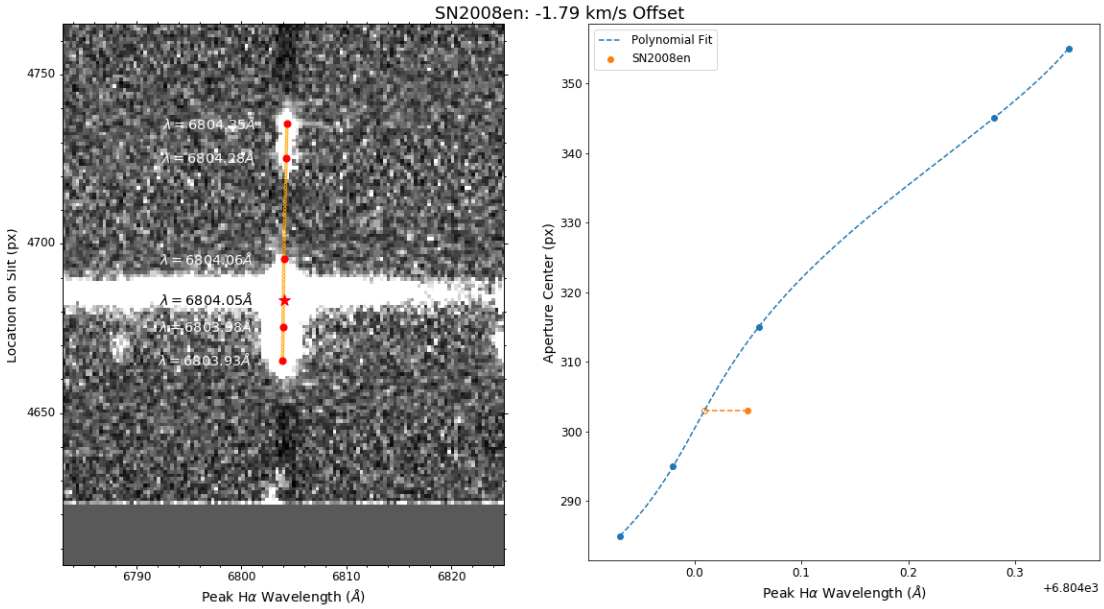

Figure B.2: SN 2008en Hα relative to host galaxy

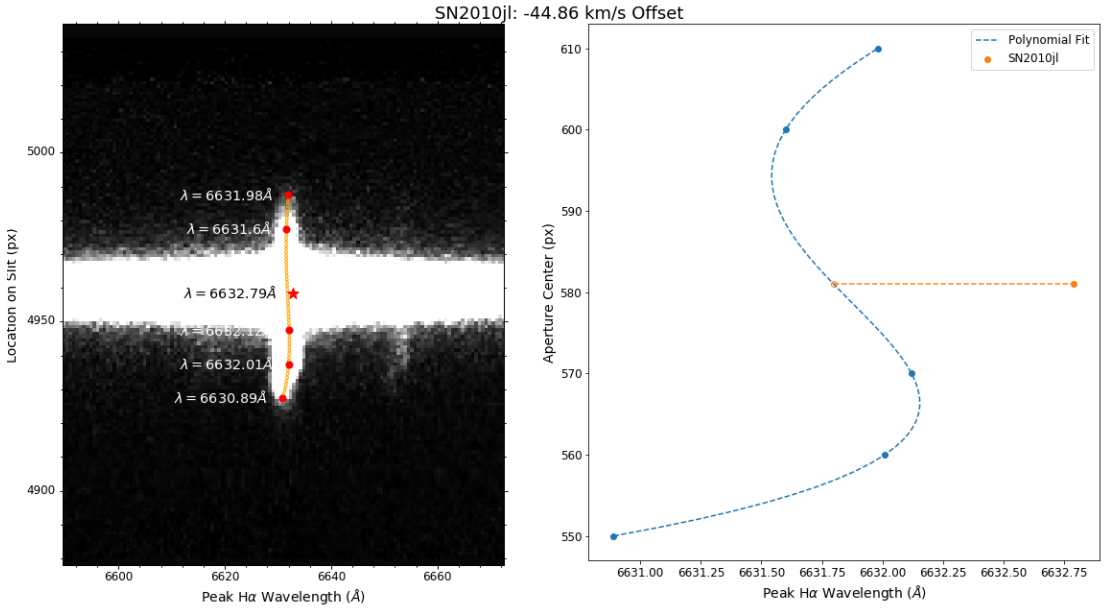

Figure B.3: SN 2010jl Hα relative to host galaxy

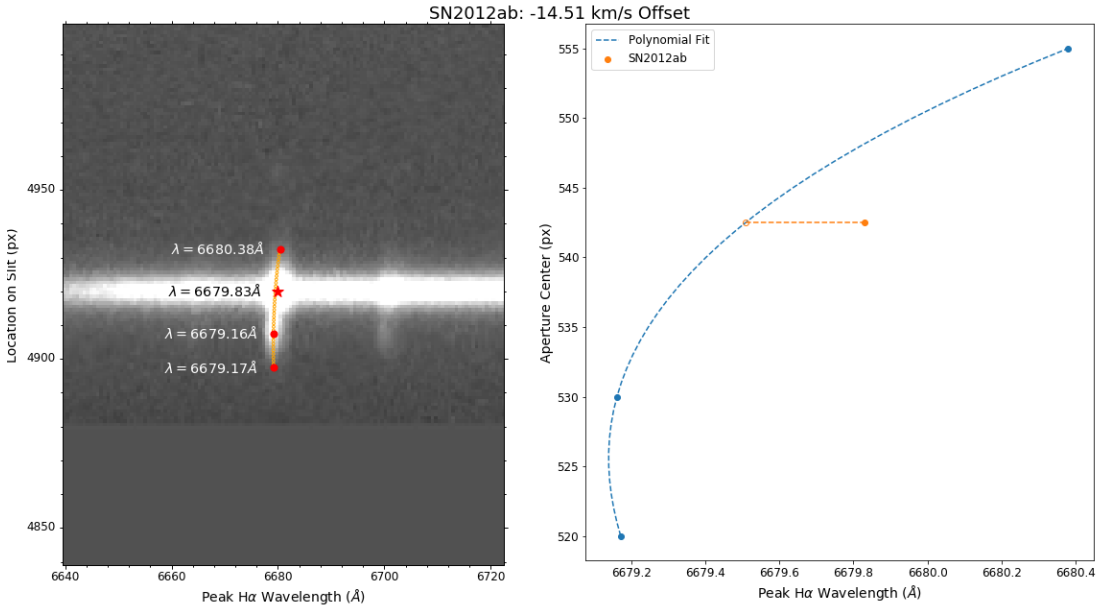

Figure B.4: SN 2012ab Hα relative to host galaxy

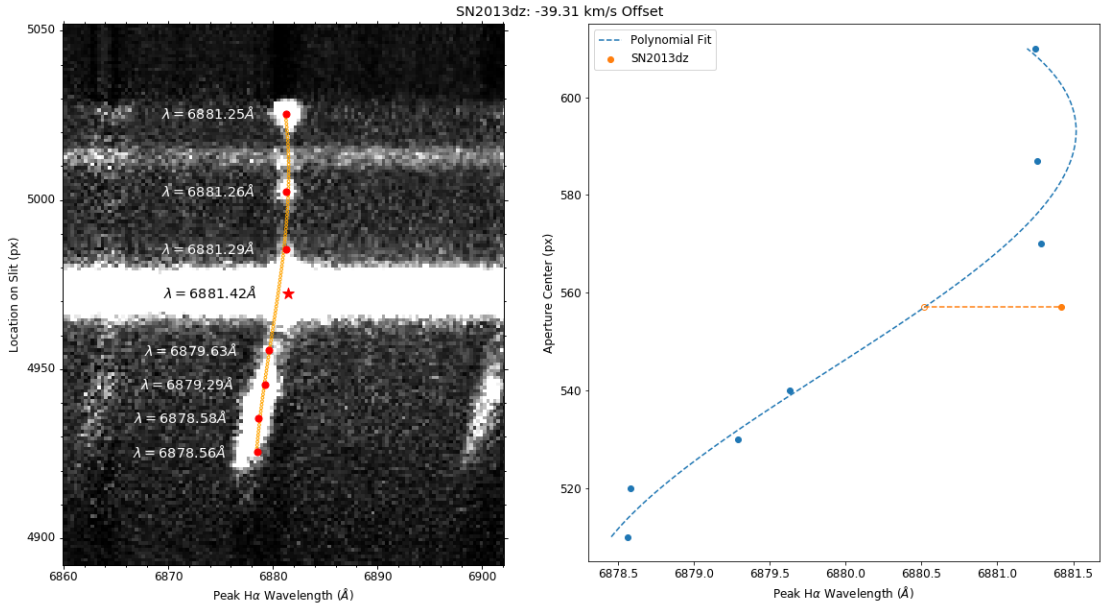

Figure B.5: SN 2013dz Hα relative to host galaxy

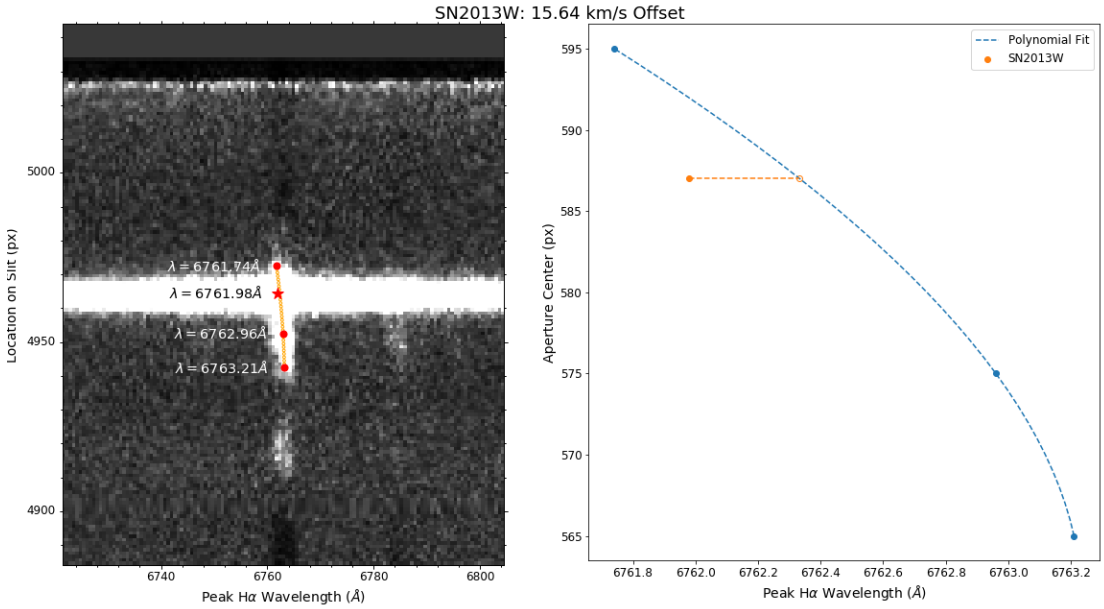

Figure B.6: SN 2013W Hα relative to host galaxy